DOI:10.1021/jf1005885

JOURNAL OF AGRICULTURAL AND FOOD CHEMISTRY
ARTICLE

Characterization of Metabolism and *in Vitro* Permeability Study of Notoginsenoside R1 from Radix Notoginseng

Jian-Qing Ruan, Weng-Im Leong, Ru Yan,* and Yi-Tao Wang

Institute of Chinese Medical Sciences, University of Macau, Taipa, Macau SAR, China

As a main and characteristic constituent in Radix notoginseng, the fate of notoginsenoside R1 (NGR1) in human is largely unknown. The present study investigated, for the first time, NGR1 metabolism by human intestinal bacteria and liver subcellular fractions, and permeability properties of NGR1 and resultant metabolites on a Caco-2 model. Samples were qualitatively analyzed using HPLC−MS/MS and quantitatively determined using HPLC−UV. When incubated with pooled human intestinal bacteria anaerobically, NGR1 showed biphasic elimination: an insignificant decrease in the first 8 h followed by a rapid elimination during 8−48 h. Four metabolites, three unambiguously identified as ginsenosides Rg1, F1 and 20(*S*)-protopanaxatriol formed via stepwise deglycosylation, and one tentatively assigned as a dehydrogenated protopanaxatriol with transformation occurring at the tetracyclic triterpenoid skeleton, were produced sequentially. Rg1 and F1 were formed transiently at low apparent velocities, while 20(*S*)-protopanaxatriol was the major metabolite with a formation rate close to the rate of NGR1 elimination and a low elimination rate. NGR1 remained intact in human liver S9 or microsomes over 1 h. Transport study of NGR1 and its metabolites revealed an ascending permeability order with stepwise deglycosylation. Taken together, the results revealed a determinant role of intestinal bacteria in the overall disposition and potential bioactivity of NGR1 in human.

KEYWORDS: Radix notoginseng; notoginsenoside R1; permeability; metabolism; intestinal bacteria; Caco-2

INTRODUCTION

Radix notoginseng (Chinese name Tienchi or Sanqi) is the dried root of *Panax notoginseng* (Burk.) F. H. Chen, an herb noted for its blood circulation promotion, blood stasis removal and pain alleviation effects, and has been widely utilized for the prevention and treatment of microcirculatory disturbance in China and other Asian countries for many years (*1*). Radix notoginseng is classified as a functional food in China (*2*), and in the United States and European countries various Radix notoginseng based herbal products are available on the market as dietary supplements.

Similar to *P. ginseng* C. A. Meyer (Asian ginseng) and *P. quinquefolius* L. (American ginseng), *P. notoginseng* belongs to the *Ginseng* genus and contains protopanaxadiol (PPD)- and protopanaxatriol (PPT)-type saponins as its main components (*3*−*5*). Notoginsenoside R1 (NGR1, **Figure 1**) is one of the PPT-type saponins in *P. notoginseng*. Compared to other *Ginseng* herbs, *P. notoginseng* contains NGR1 in much more substantial amount (*5*). Thus, NGR1 is widely adopted as the characteristic marker of *P. notoginseng* when distinguishing this herb from other *Ginseng* herbs and evaluating quality of Radix notoginseng or related products (*3*−*6*). Extensive pharmacological evaluation of NGR1 has been conducted on both *in vivo* and *in vitro* models. NGR1 has exhibited various health promotion activities, including neuroprotective (*7*), hepatic protective (*8*), cardiovascular protective (*9*, *10*), and immune stimulation effects (*11*). Therefore, NGR1 was considered as one of the main bioactive ingredients contributing to beneficial effects of Radix notoginseng and documented in China Pharmacopoeia as the chemical marker for quality control of this herb (*12*).

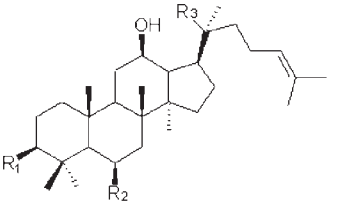

Saponins	R_1	R_2	R_3
Notoginsenoside R1	OH	Oglc(2-1)xyl	Oglc
Ginsenoside Rg1	OH	Oglc	Oglc
Ginsenoside F1	OH	OH	Oglc
Protopanaxatriol	OH	OH	OH

Figure 1. Chemical structures of notoginsenoside R1 and its main metabolites formed by human intestinal bacteria; glc, glucose; xyl, xylose.

In contrast to the well-defined beneficial actions, so far, the information on the absorption, distribution, metabolism and

*To whom correspondence should be addressed. E-mail: ruyan@umac.mo. Tel: 853-83974876. Fax:853-28841358.

 Published on Web 04/21/2010

excretion (ADME) properties and consequently the *in vivo* fate of NGR1 is surprisingly limited. Recent studies with Radix notoginseng extract revealed a very low oral bioavailability (< 10%) of NGR1 in the rat (*13*−*15*). However, the oral pharmacokinetic property of individual NGR1 in human remains to be addressed. On the basis of the existing reports on other PPD- and PPT-type saponins, a poor permeability in the gut and an extensive hydrolysis in the intestinal tract of NGR1 are anticipated after oral dosing, thus leading to a low oral bioavailability. On the other hand, it is widely accepted that, when taken orally, ginsenoside metabolites formed by intestinal bacteria, instead of the parent saponins, reach the systemic circulation easier and hence exert beneficial effects (*16*, *17*). However, so far, there is little evidence supporting this speculation in the case of NGR1. Moreover, the role of the liver, the principal site of biotransformation of most drugs, in the *in vivo* process of NGR1 is still unclear.

Therefore, the present study was designed to (1) characterize NGR1 hydrolysis by human intestinal bacteria, qualitatively and quantitatively; (2) determine and compare the permeability properties of NGR1 and metabolites generated by intestinal bacteria on a Caco-2 monolayer model; and (3) examine metabolic stability of NGR1 in human liver with S9- and microsome-based incubation systems.

MATERIALS AND METHODS

Materials. Notoginsenoside R1 (purity >95%) was supplied by Kuiqing Trading Co. Ltd. (Tianjin, China). Ginsenoside F1 (purity >98%) and 20(*S*)-protopanaxatriol (PPT) (purity >98%) were purchased from National Institute for the Control of Pharmaceutical and Biological Products (Beijing, China). Ginsenoside Rg1 and Rb1 were isolated from Radix notoginseng in our institute with purities >95% by HPLC analysis. BBL brain heart infusion (BHI) medium, GasPak EZ Anaerobe Container System with Indicator and GasPak EZ Large Incubation Container were purchased from Becton Dickinson (Franklin Lakes, NJ). L-Cystine was from Research Organics, Inc. (Cleveland, OH). Hanks' balanced salt solution (HBSS), rhodamine 123, collagen type I from rat tail, sodium pyruvate, dimethyl sulfoxide (DMSO), hemin bovine and vitamin K1 were supplied by Sigma-Aldrich (St. Louis, MO). Methanol, 1-butanol and acetonitrile were HPLC-grade from Merck (Darmstadt, Germany). Deionized water was purified by a Milli-Q purification system (Millipore; Bedford, MA). Dulbecco's modified Eagle's medium (DMEM), fetal bovine serum (FBS), 0.25% trypsin−EDTA, penicillin−streptomycin solution and nonessential amino acids were purchased from GibcoBRL Life & Technologies (Grand Island, NY). Transwell plates (12-well, 0.4 μm pore size, 1.12 cm^2, polycarbonate filter) were purchased from Corning Costar Co (Cambridge, MA). Caco-2 cells were obtained from the American Type Culture Collection (Rockville, MD). Pooled human liver S9 and microsomes were supplied by Sigma.

Preparation of Human Intestinal Bacteria. The culture medium was modified from the method reported by Chang and Nair (*18*). In brief, 100 mL of autoclaved BHI medium (3.7 g/100 mL) was supplemented with 0.05 mg of vitamin K1, 0.5 mg of hemin bovine and 50 mg of L-cystine. Fresh fecal samples from healthy Chinese volunteers (20−32 years) were provided by Kiang Wu hospital (Macau, China) according to a protocol approved by the Medical Department, Kiang Wu Hospital and the Internal Ethical Committee of the Institute of Chinese Medical Sciences, University of Macau. Five fecal samples (2 g of each) were pooled together and mixed well with 30 mL of culture medium. The resultant fecal suspension was centrifuged at 200*g* for 5 min and supernatant decanted and centrifuged at 5000*g* for 30 min. The resultant precipitate was resuspended with 10 mL of BHI medium to produce intestinal microflora solution.

Metabolism of NGR1 by Human Intestinal Bacteria. The biotransformation of NGR1 by human intestinal bacteria was determined in a 5 mL incubation system containing 250 μL of intestinal microflora solution and 100 μL of NGR1 stock solution in DMSO (NGR1 final concentration 0.2 mM) in BHI medium. The incubation system was anaerobically incubated at 37 °C in a GasPak EZ Anaerobe Pouch System for 0, 4, 8, 12, 15, 18, 21, 24, 36, 48, and 72 h, respectively. Zero-minute incubations or reactions without microflora solution or NGR1 served as controls. Each reaction was performed 3 times. Reactions were stopped by addition of 2 mL of ice-cold 1-butanol followed by immediate centrifugation at 5000*g* for 30 min to remove the bacteria. After adding 100 μL of ginsenoside Rb1 (10 mM) as internal standard, the sample was twice extracted with 10 mL of water saturated 1-butanol. The organic fractions was combined and evaporated under N_2 at 37 °C. The residue were then reconstituted with 200 μL of methanol, filtered through a 0.45 μm membrane filter before being subjected to HPLC analysis.

Calibration Curves of NGR1, Ginsenosides Rg1, F1 and PPT in Human Intestinal Bacterial Incubation System. Stock solutions of NGR1, Rg1, F1 and PPT were prepared and diluted to appropriate concentrations with DMSO for construction of calibration curves. Each calibration curve contained 6 different concentrations and was performed in triplicate. An aliquot (100 μL) of stock solutions of each compound at different concentrations was mixed with 4.9 mL of BHI medium containing 100 μL of human microflora solution prepared as described above. The resultant samples were processed immediately as described above. The calibration curves were constructed by plotting the peak area ratio of the spiked analyte to internal standard as a function of the concentration of each analyte. The limits of detection (LOD) and quantification (LOQ) under the present chromatographic conditions were determined at a signal-to-noise ratio (S/N) of above 3 and 10, respectively.

Metabolic Stability of NGR1 in Human Hepatic Subcellular Fractions. The metabolic stability of NGR1 in human liver subcellular fractions was determined in a total of 200 μL of reaction solution containing NGR1 (final concentration 0.2 mM), human liver S9 or microsomes (1 mg/mL), NADPH-regenerating system (4 mM of $MgCl_2$, 1 mM $NADP^+$, 1 mM glucose-6-phosphate and 1 U/mL glucose-6-phosphate dehydrogenase) and 100 mM potassium phosphate buffer (pH 7.4). Reactions were conducted at 37 °C for 60 min. The incubation systems with denatured liver S9 or microsome or without NADPH-regenerating system served as controls. All the experiments were performed in triplicate. Reactions were terminated by adding 200 μL of methanol and vortexing to mix thoroughly. After centrifugation at 15000*g* for 5 min, the resultant supernatant was filtered through a 0.45 μm membrane filter and an aliquot (70 μL) applied to an HPLC−DAD system or an HPLC−MS/MS system.

Culture of Caco-2 Cells. Caco-2 cells obtained from the American Type Culture Collection at passage 30−40 were cultured in DMEM supplemented with 10% fetal bovine serum and 1% nonessential amino acids, at 37 °C in an atmosphere of 5% CO_2 and 90% relative humidity. Cells were subcultured at 80−90% confluence by trypsinization with 0.05% trypsin−EDTA. In transport studies, Caco-2 cells (at passages 30−50) were seeded on 12-well plates at a density of 1×10^5 cells/well and cultured for 21 days before starting transport study. For each experiment, the integrity of the monolayer was monitored by measuring the transepithelial electrical resistance (TEER) (*19*) with an epithelial voltohmmeter (World Precision Instruments, Inc., FL) and the permeability of the paracellular marker lucifer yellow. Only Caco-2 monolayers with TEER above 300 $\Omega\ cm^2$ before and after the transport study and a leakage rate of lucifer yellow less than 1% per hour were utilized in the transport study. The efflux transporter P-glycoprotein (P-gp) functionality in Caco-2 monolayers was validated using the P-gp probe substrate rhodamine 123. Rhodamine 123 (5 μM) exhibited substantial directional preference with an efflux ratio of 39.4, suggesting the normal presence of P-gp transporter in the Caco-2 cell monolayers used.

Transport of NGR1, Ginsenosides Rg1, F1 and PPT across Caco-2 Cell Monolayer. Prior to the transport study, cytotoxicity of NGR1, ginsenoside Rg1, F1 and PPT toward Caco-2 cells was determined using MTT assays. Non-cytotoxic concentrations of NGR1 (1 mM), Rg1 (1 mM), F1 (200 μM) and PPT (50 μM) were chosen for transport study.

Transport study was carried out in HBSS buffer. After 21 days of culture, the prepared Caco-2 monolayers were rinsed twice with HBSS and preincubated in HBSS at 37 °C for 30 min. In the absorption transport study, 0.5 mL of HBSS solutions containing NGR1, Rg1, F1 or PPT was loaded at the apical (A) side (donor chamber), and 1.5 mL of blank HBSS was placed at the basolateral (B) side (receiver chamber). In the secretion transport study, 1.5 mL of the HBSS containing test compound was added at the B side (donor chamber) and 0.5 mL of blank HBSS was placed at the A side (receiver chamber). Aliquots of 0.1 mL were taken from receiver

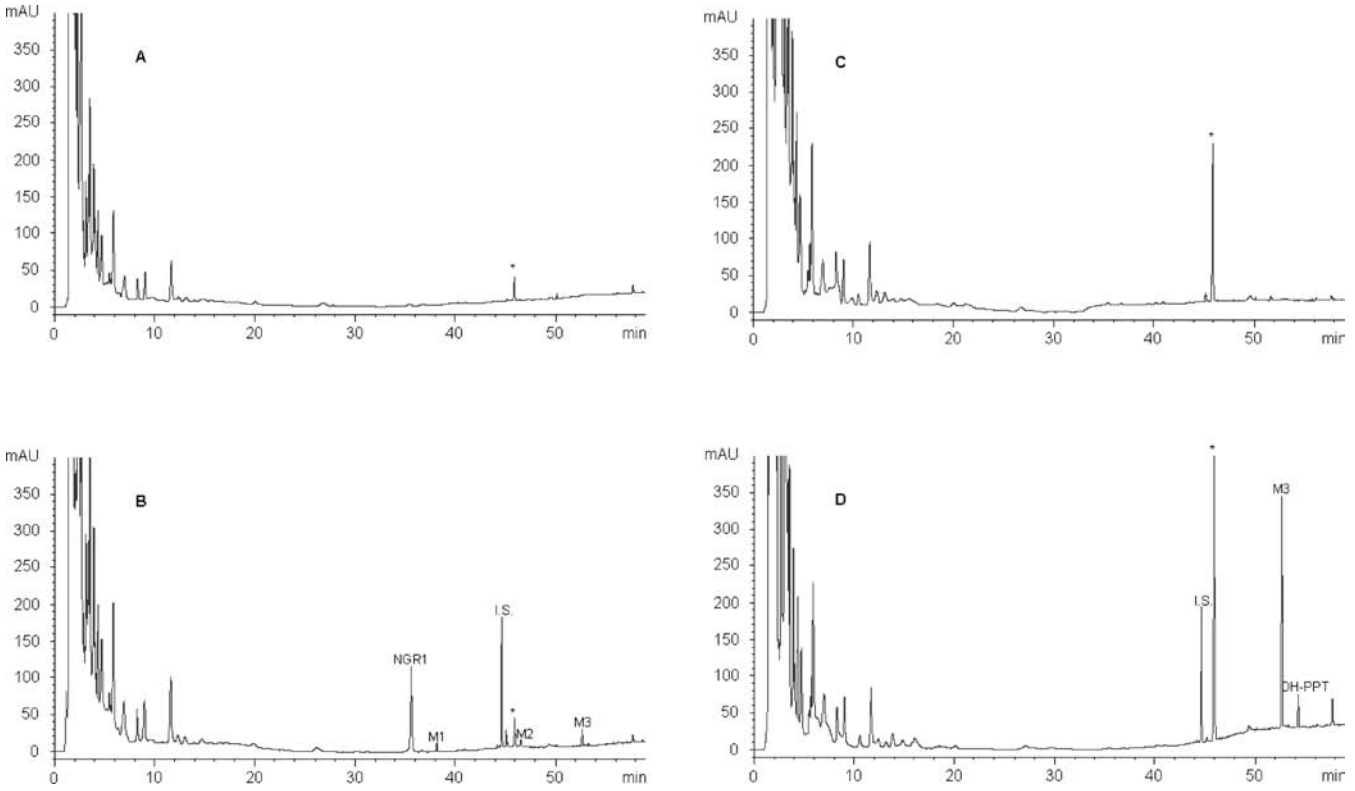

Figure 2. Typical HPLC chromatograms of (**A**) 12 h control reaction without NGR1, (**B**) 12 h reaction with NGR1, (**C**) 48 h control reaction without NGR1, (**D**) 48 h reaction with NGR1. *: impurity detected in the incubation system with time prolonged.

chambers at different time intervals (0, 30, 60, 90, 120 min) for HPLC analysis. After each sampling, 0.1 mL of HBSS was added to the receiver chamber to maintain a constant volume. At the last time point, 0.1 mL of sample was also withdrawn from the donor chamber for HPLC analysis to calculate the recovery. All the experiments were performed three times in duplicate.

The apparent permeability coefficients (Papp) of NGR1, Rg1, F1 and PPT from apical side to basolateral side ($Papp_{A\rightarrow B}$) or from basolateral side to apical side ($Papp_{B\rightarrow A}$) in bidirectional transport study on Caco-2 cell model were calculated using the following equation as reported previously (*20*):

$$\text{Papp} = (\mathrm{d}C/\mathrm{d}t \times V)/(C_0 \times A)$$

where $\mathrm{d}C/\mathrm{d}t$ is the rate of the test compound appearing in the receiver chamber, V is the volume of the solution in the receiver chamber, C_0 is the initial concentration of the test compound added in the donor chamber, and A is the cell monolayer surface area.

Efflux ratio ($Papp_{B\rightarrow A}/Papp_{A\rightarrow B}$) >2 was adopted when determining whether efflux transporter(s) was involved in transport of the test compound.

HPLC−DAD Analysis. Quantitative analysis was completed on an Agilent series 1200 HPLC apparatus (Agilent Technologies, Santa Clara, CA) equipped with a vacuum degasser, a binary pump, an autosampler and a diode array detector. An Alltech Alltima C_{18} column (250 mm × 4.6 mm, 5 μm) was used. The column temperature was maintained at 25 °C. The flow rate was 1.5 mL/min. Injection volume was 5 μL of samples from intestinal bacterial metabolic studies and 70 μL of other samples. NGR1, ginsenosides Rg1, F1 and PPT were monitored at 203 nm, and their UV absorption was recorded over 210−400 nm. The mobile phase consisted of water (A) and acetonitrile (B), and a gradient elution was adopted as follows: 0−30 min, 18−19% B; 30−40 min, 19−31% B; 40−60 min, 31−100% B.

HPLC−MS/MS Analysis. Structural identification was performed on an LC/MSD ion trap system (Agilent Technologies, Palo Alto, CA) consisting of an HP 1100 series binary pump HPLC system and an ion-trap mass spectrometer with an electrospray ionization interface, connected to an Agilent ChemStation software. The mobile phase consisted of 50 mM ammonium acetate in water (A) and acetonitrile (B). The gradient was the same as described above in the section HPLC−DAD Analysis. ESI-MS analyses were operated in both positive and negative ionization modes. Negative ion mode provided higher sensitivity, better reproducibility and less interference from the incubation system under the present analytical conditions and, thus, was chosen for sample analysis in the present study. The detailed conditions for negative ionization mode were as follows: drying gas N_2 8 L/min, temperature 325 °C, pressure of nebulizer 30 psi, capillary voltage −3500 V, scan range 100−1400 m/z. ESI-MS/MS conditions were as follows: negative ion mode, separation width 4, fragment amplification 1.0, scan range 100−1400 m/z.

Data Analysis. All data were expressed as mean ± standard deviation (SD). Difference between permeability of NGR1 and its metabolites was assessed using unpaired Student's t-test. A $p < 0.05$ value was deemed significant for all tests.

RESULTS

Metabolism of Notoginsenoside R1 by Human Intestinal Bacteria. When NGR1 was incubated with pooled human intestinal bacteria, the peak of NGR1 decreased with time and several additional peaks were observed within 72 h incubation (**Figure 2**). When compared with controls (a mixture of NGR1 with intestinal bacteria without incubation, incubations without NGR1, and NGR1 in BHI medium alone without bacteria), four of these unknown peaks were identified as metabolites of NGR1 with retention times of 38.1 min (M1), 46.5 min (M2), 52.6 min (M3) and 54.3 min (M4) (**Figures 2B** and **2D**).

The structures of M1, M2 and M3 were unambiguously identified as ginsenoside Rg1, F1 and 20(*S*)-protopanaxatriol (PPT) by comparison of their retention times, UV spectra and mass spectra (MS^1 and MS^2) with those of the authentic compounds. As shown in **Figure 3**, the mass spectrum of M1 showed the pseudo molecular ion $[M - H]^-$ at m/z 799, which was 132 mass units less than that of NGR1 (m/z 931) corresponding to the loss of one xylose, and the acetoxy adduct ion $[M + AcO]^-$ at m/z

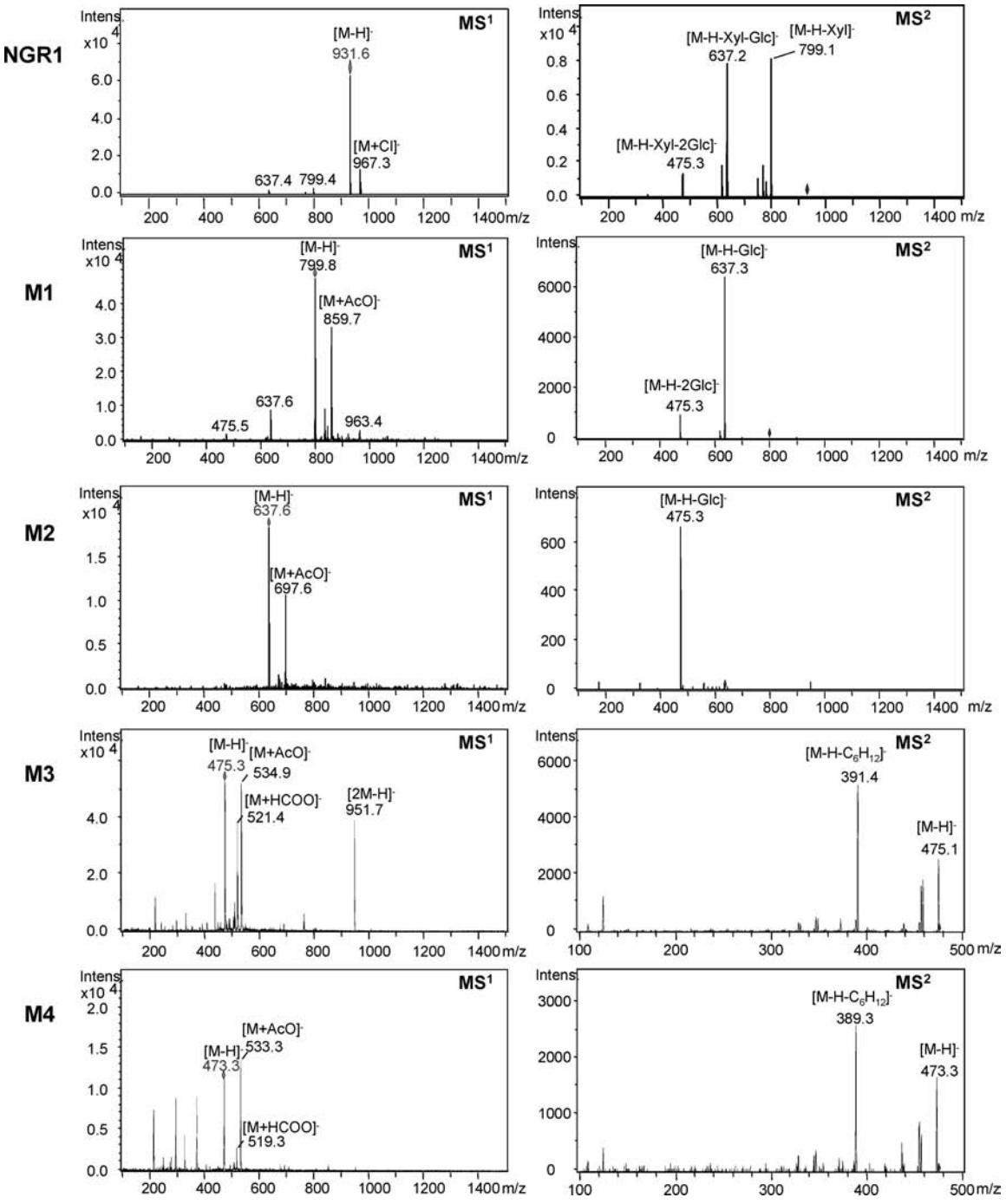

Figure 3. MS^1 and MS^2 data of NGR1 and its metabolites formed by human intestinal bacteria. M1: ginsenoside Rg1. M2: F1. M3: PPT. M4: DH-PPT.

859. Its MS/MS data showed ions at m/z 637 ($[M - H - Glc]^-$) and m/z 475 ($[M - H - 2Glc]^-$), the same as those observed with standard ginsenoside Rg1. In addition, the retention time and the UV spectrum of M1 were also identical to those of ginsenoside Rg1. Thus, M1 was identified as ginsenoside Rg1. The characteristic ions at m/z 637 ($[M - H]^-$) and m/z 697 ($[M + AcO]^-$) in the mass spectrum of M2 indicated that this metabolite has a molecular weight of 638 Da, which corresponded to loss of one glucose from ginsenoside Rg1. Its UV and MS/MS spectra were identical to those of F1 and Rh1 while the retention time was the same as that of F1 but different from that of Rh1. Therefore M2 was assigned as F1. The mass spectrum of M3 showed its $[M - H]^-$ ion at m/z 475, $[M + HCOO]^-$ ion at m/z 521, $[M + AcO]^-$ ion at m/z 535 and $[2M - H]^-$ ion at m/z 951, indicating a molecular weight of 476 Da corresponding to further loss of one glucose from F1. Its MS/MS spectrum also exhibited a characteristic ion at m/z 391 ($[M - H - C_6H_{12}]^-$) resulting from the neutral loss of the aliphatic side chain at C20 position. Moreover, the retention time and UV spectrum of M3 were the same as those of 20(*S*)-protopanaxatriol. Thus, M3 was identified as 20(*S*)-protopanaxatriol (PPT).

The identity of M4 was only tentatively assigned due to lack of the standard compound. Mass spectrum of M4 exhibited characteristic ions at m/z 473 ($[M - H]^-$), m/z 519 ($[M + HCOO]^-$) and m/z 533 ($[M + AcO]^-$), all 2 mass units less than those of PPT, indicating a dehydrogenated product of PPT. Furthermore, the appearance of M4 was later than PPT. Therefore, M4 was tentatively identified as a dehydrogenated product of PPT. Similar to PPT, the characteristic ion at m/z 389 corresponding to the loss of the aliphatic side chain ($[M - H - C_6H_{12}]^-$) was

Table 1. Calibration Curves for NGR1 and Its Metabolites

		$y = ax + b$				
compd	retention time (min)	slope (a)	intercept (b)	r^2	concn range (μM)	detection limit (μM)
NGR1	35.6	12.227	0.161	0.9999	2.2−280.0	0.41
Rg1	38.1	14.884	0.010	0.9998	2.2−280.0	0.48
F1	46.5	18.925	0.091	0.9996	1.4−87.5	0.39
PPT	52.6	18.657	0.009	1.0000	2.5−320.0	0.40

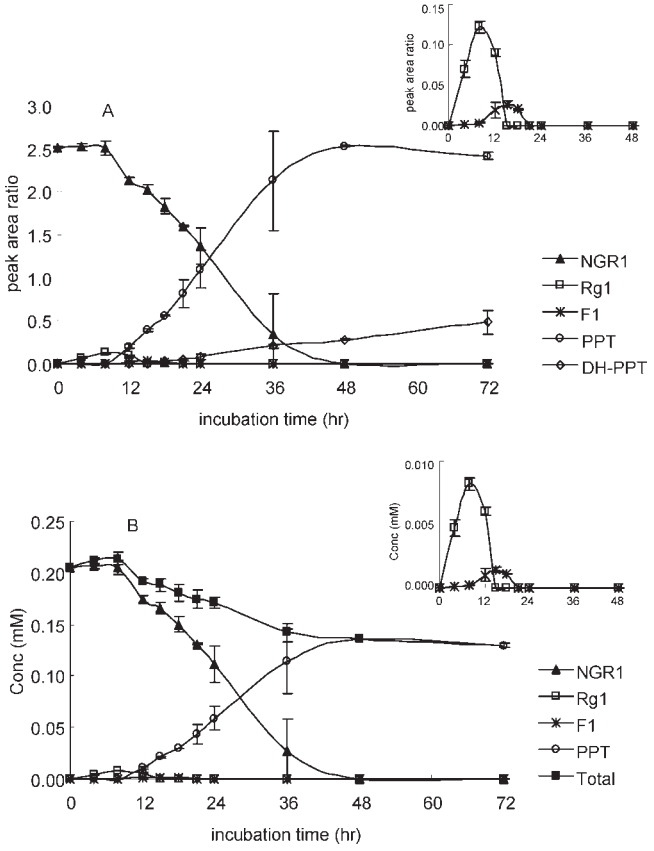

Figure 4. Time courses of NGR1 metabolism and metabolite generation by human intestinal bacteria. **A**: Peak area ratio−time plot. **B**: Concentration−time plot.

observed, indicating that the dehydrogenation of PPT occurred on the tetracyclic triterpenoid skeleton.

Time Course of NGR1 Metabolism by Human Intestinal Bacteria. As shown in **Figure 2**, NGR1 and its metabolites were eluted with baseline separation under the present chromatographic condition. The calibration curves (**Table 1**) for NGR1, ginsenoside Rg1, F1 and PPT provided good linearity ($r^2 > 0.998$) over the concentration ranges tested. The detection limits were 0.4 μM (NGR1, F1 and PPT) and 0.5 μM (Rg1) (**Table 1**).

The time courses of NGR1 metabolism and metabolite generation by human intestinal bacteria are shown in **Figure 4**. During the first 8 h, NGR1 decreased very slowly (average velocity: 0.18 μmol/h) with >97% remained at 8 h, whereas it was eliminated rapidly (average velocity: 4.17 μmol/h) afterward and disappeared from the reaction system 48 h after incubation. Rg1 and F1 reached their maximum at 8 and 15 h respectively and then were eliminated rapidly, whereas PPT was not detected until 8 h, reached its maximum at 48 h (average velocity over 8−48 h: 3.40 μmol/h) and decreased slowly afterward with a slow increase of the dehydrogenated metabolite M4 (**Figure 4**). Great variations

Table 2. Apparent Permeability Coefficients (Papp) of NGR1 and Its Metabolites Determined on the Caco-2 Model[a]

compd	$Papp_{A\rightarrow B}$ ($\times 10^{-6}$ cm/s)	$Papp_{B\rightarrow A}$ ($\times 10^{-6}$ cm/s)	$Papp_{B\rightarrow A}/Papp_{A\rightarrow B}$
NGR1	0.088 ± 0.010	0.093 ± 0.011	1.05
Rg1	$0.236^{***} \pm 0.017$	$0.244^{***} \pm 0.017$	1.03
F1	$0.866^{\#\#} \pm 0.220$	$4.523^{\#\#\#} \pm 2.06$	5.22
PPT	$18.170^{\xi\xi\xi} \pm 0.942$	$18.720^{\xi\xi\xi} \pm 2.417$	1.03

[a] Data are presented as means ± SD (n = 3). $^{***}p < 0.001$, $^{\#\#}p < 0.01$ and $^{\#\#\#}p < 0.001$, $^{\xi\xi\xi}p < 0.001$ as compared to the corresponding values for NGR1, Rg1 and F1, respectively.

were observed in the amounts of NGR1 left and PPT generated at 36 h due to a variation in NGR1 hydrolyzing rates over 8−48 h. When the amounts of ginsenosides Rg1, F1 and PPT generated were calculated and compared based on 1:1 stoichiometric conversion, the metabolites at their maximum levels accounted for 6.3% (Rg1), 1.1% (F1) and 71.0% (PPT) of initial NGR1, respectively. Furthermore, the total recovery of the compound per se and the metabolites ginsenosides Rg1, F1 and PPT formed before the advent of DH-PPT reached >95%. All these data supported that NGR1 was stepwisely deglycosylated mainly through the following pathway: NGR1 → Rg1 → F1 → PPT.

Metabolism of NGR1 by Human Hepatic Subcellular Fractions. When incubated with human liver S9 fraction or microsomes in the absence or presence of NADPH-regenerating system for 1 h, NGR1 remained intact and the recovery of NGR1 reached 98 ± 1.5% (S9) and 97 ± 2.8% (microsome), respectively. Furthermore, HPLC−MS/MS analysis revealed no phase I transformation of NGR1.

Transport of NGR1 and Its Main Metabolites across Caco-2 Monolayer. The bilateral Papp values for NGR1 and its metabolites across Caco-2 cell monolayers are summarized in **Table 2**. With stepwise removal of glycosyl groups, the Papp values ($Papp_{A\rightarrow B}$ value in the case of F1) of the metabolites increased. NGR1 exhibited a very low Papp value ($\times 10^{-8}$ cm/s), indicating a very poor oral absorption (<1%) in human body. The Papp values ($\times 10^{-7}$ cm/s) of ginsenosides Rg1 and F1 (A to B side) were 1 order of magnitude higher than that of NGR1, while PPT showed a Papp ($\times 10^{-5}$ cm/s) that was 2 orders of magnitude higher than that of Rg1 and F1 (A to B side), indicating an increasing permeability. The efflux ratios ($Papp_{B\rightarrow A}/Papp_{A\rightarrow B}$) of NGR1, Rg1, and PPT were within the range of 1.0−1.5, suggesting that there was no significant difference between the permeability in the A to B and that in the B to A directions and NGR1, ginsenosides Rg1, and PPT transport across intestinal epithelial cells mainly through passive diffusion, whereas the transport of F1 from B to A direction was significantly higher than that obtained from A to B direction and the efflux ratio was 5.22, indicating that F1 might be the substrate of efflux transporter(s).

DISCUSSION

In the past decade, people have attributed the beneficial effects of many ginsenosides to their metabolites formed in the gastrointestinal tract when taken orally. Although degradation pathways of many ginsenosides have been well examined *in vivo* and *in vitro* using animals (*15*−*17*, *21*−*23*), information in human is sparely available.

As the characteristic constituent and the chemical marker of Radix notoginseng, NGR1 exhibited diverse beneficial effects. However, its ADME properties and hence its biologically active form(s) are still unclear. In the present study, NGR1 metabolism by human intestinal bacteria and human liver subcellular fractions were investigated, for the first time, to predict its disposition in humans.

Four metabolites appeared stepwisely when NGR1 was incubated with different pooled human intestinal bacteria, three of which were unambiguously identified as ginsenoside Rg1, F1 and 20(*S*)-protopanaxatriol by comparison of their retention times, UV spectra and MS spectra with those of standards. The initial colonic deglycosylation of NGR1 occurred preferentially at C6 to yield Rg1. The resultant Rg1 could further remove one molecule of glucose either at C-6 to generate F1 or at C-20 to have Rh1. In previous reports on Rg1 hydrolysis by rat intestinal bacteria, both Rh1 and F1 formations were speculated, although no definite evidence was provided to support Rh1 formation. Other studies support that acidic hydrolysis of Rg1 in the stomach generated Rh1 while F1 was formed from Rg1 by intestinal bacteria (*21*,*22*). In the present study, existence of Rh1 in the human intestinal bacterial incubation system was ruled out using Rh1 standard.

Another metabolite M4, which was tentatively identified as a dehydrogenated PPT (DH-PPT) based on MS analyses, was detected 18 h after incubation. To the best of our knowledge, this is the first report of dehydrogenation of PPT by human intestinal bacteria. The dehydrogenation position was on the tetracyclic triterpenoid skeleton as evidenced by the characteristic ion of the core structure of M4 two mass units less than that of PPT, thus M4 might be formed via carbonylation at C3, C6 or C12. However, in a recent report from Yang et al., a dehydrogenated PPT was detected in rat urine when ginsenoside Re was administered and the authors speculated a dehydrogenation at the aliphatic side chain of PPT on basis of similar MS/MS data (*23*). The absolute structure of DH-PPT, its production *in vivo* and biological activities are worthy of investigation.

The appearance and elimination of Rg1 and F1 were rapid and their quantities detected in the incubation system were relatively low (**Figure 4**). Furthermore, PPT formation rate was around 80% of NGR1 elimination rate (3.40 μmol/h vs 4.17 μmol/h) over the period of 8−48 h, indicating that, once formed, Rg1 was further transformed to F1 and then F1 to PPT very rapidly. PPT was the most abundant metabolite after 12 h and reached > 70% of initial NGR1 at 48 h. PPT is the end metabolite of PPT-type ginsenosides via stepwise deglycosylation. PPT exhibited anti-angiogenic, radiation-protective and antioxidation effects (*22*−*26*), and over 80% of PPT entered the circulation (*27*), supporting its important role *in vivo*.

It is very interesting to note that there were at least two phases of NGR1 elimination by human intestinal bacteria. In phase 1 (within the first 8 h of incubation), NGR1 was slowly deglycosylated at an average velocity of 0.18 μmol/h. While in phase 2 (during 8−48 h), NGR1 disappeared from the system rapidly at an average velocity (4.17 μmol/h) > 20 times of phase 1. The apparent biphasic elimination was also observed with another PPT-type ginsenoside Rg1 while absent with the PPD-type ginsenoside Rb1, which showed an immediate rapid elimination in human intestinal bacteria (our group unpublished data). This might attribute to different intestinal microflora that are involved in biotransformation of PPD- and PPT-type ginsenosides (*28*). The mechanism governing the biphasic deglycosylation of NGR1 by human intestinal bacteria warrants further investigation.

Recent reports reveal that, in addition to the deglycosylation in gastrointestinal tract, phase I metabolism also plays a role, but to different extents, in *in vivo* fates of some ginsenosides (*15*,*29*). Lai et al. (*29*) identified two mono-oxygenated metabolites of ginsenoside Rh1 *in vivo* after intragastrical administration and oxidation caused about 75% Rh1 loss within 30 min in rat hepatic S9 and microsomes. The monooxidized metabolite of Rg1 detected in rat bile and urine only accounted for 0.2% and 0.1% of its oral dose, respectively (*15*). In the case of NGR1, the observation that NGR1 was mainly eliminated via biliary excretion in its intact form supports its high resistance to hepatic metabolism in the rat (*15*). In the present study, there was no evidence supporting significant biotransformation of NGR1 in human liver microsomes. These results imply that hepatic metabolism, if any, plays an insignificant role in NGR1 disposition.

The transport of the main metabolites of NGR1 across Caco-2 cell monolayer was compared with the parent compound in parallel. Our data showed a low permeability of NGR1 across Caco-2, suggesting a poor absorption (< 1%) in human after taken orally. This result was in good agreement with the low oral bioavailability (0.2−0.6%) of NGR1 in rats reported recently (*15*), indicating a determinant role of NGR1 permeability in its oral bioavailability. Metabolites formed by human intestinal bacteria exhibited higher permeability than NGR1 in the following increasing order: PPT > F1 > Rg1 > NGR1 (**Table 2**). These findings suggest that the metabolites formed by intestinal bacteria may have better absorption and thus might be the main *in vivo* forms when NGR1 is taken orally. Since other factors including solubility, biliary excretion, acidic hydrolysis in gastric juice may also affect the oral bioavailability of PPT- and PPD-type ginsenosides, *in vivo* study is warranted to determine the bioavailability of NGR1 and its main drug-related forms after oral dosing.

The present study revealed that NGR1 has poor permeability, no hepatic biotransformation, yet extensive hydrolysis by intestinal bacteria in gut lumen via NGR1 → Rg1 → F1 → PPT → DH-PPT using human-derived *in vitro* models. The resultant deglycosylated metabolites bear better permeability. These findings, if true *in vivo*, indicate the implications of the metabolites formed by deglycosylation in human when NGR1 is taken orally, thus calling for future investigations on their *in vivo* fates in the human body.

ABBREVIATIONS USED

NGR1, notoginsenoside R1; PPD, protopanaxadiol; PPT, protopanaxatriol; DH-PPT, dehydrogynated protopanaxatriol.

ACKNOWLEDGMENT

The authors thank Jacky Lei (the Chief of Department of Clinical Laboratory, Kiang Wu Hospital) and his colleagues for their support in feces sample collection from healthy volunteers.

LITERATURE CITED

(1) Jia, L.; Zhao, Y.; Liang, X. J. Current evaluation of the millennium phytomedicine- ginseng (II): Collected chemical entities, modern pharmacology, and clinical applications emanated from traditional Chinese medicine. *Curr. Med. Chem.* **2009**, *16*, 2924–2942.

(2) Yang, Y. X. Scientific substantiation of functional food health claims in China. *J. Nutr.* **2008**, *138*, 1199S–1205S.

(3) Wang, C. Z.; Ni, M.; Sun, S.; Li, X. L.; He, H.; Mehendale, S. R.; Yuan, C. S. Detection of adulteration of notoginseng root extract with other Panax species by quantitative HPLC coupled with PCA. *J. Agric. Food Chem.* **2009**, *57*, 2363–2367.

(4) Dong, T. T. X.; Cui, X. M.; Song, Z. H.; Zhao, K. J.; Ji, Z. N.; Lo, C. K.; Tsim, K. W. K. Chemical assessment of roots of *Panax notoginseng* in China: regional and seasonal variations in its active constituents. *J. Agric. Food Chem.* **2003**, *51*, 4617–4623.

(5) Wan, J. B.; Li, S. P.; Chen, J. M.; Wang, Y. T. Chemical characteristics of three medicinal plants of the Panax genus determined by HPLC-ELSD. *J. Sep. Sci.* **2007**, *30*, 825–832.

(6) Qian, Z. M.; Wan, J. B.; Zhang, Q. W.; Li, S. P. Simultaneous determination of nucleobases, nucleosides and saponins in *Panax notoginseng* using multiple columns high performance liquid chromatography. *J. Pharm. Biomed. Anal.* **2008**, *48*, 1361–1367.

(7) Gu, B.; Nakamichi, N.; Zhang, W. S.; Nakamura, Y.; Kambe, Y.; Fukumori, R.; Takuma, K.; Yamada, K.; Takarada, T.; Taniura, H.;

Yoneda, Y. Possible protection by notoginsenoside R1 against glutamate neurotoxicity mediated by N-methyl-D-aspartate receptors composed of an NR1/NR2B subunit assembly. *J. Neurosci. Res.* **2009**, *87*, 2145–2156.

(8) Chen, W. X.; Wang, F.; Liu, Y. Y.; Zeng, Q. J.; Sun, K.; Xue, X.; Li, X.; Yang, J. Y.; An, L. H.; Hu, B. H.; Yang, J. H.; Wang, C. S.; Li, Z. X.; Liu, L. Y.; Li; Zheng, J.; Liao, F. L.; Han, D.; Fan, J. Y.; Han, J. Y. Effect of notoginsenoside R1 on hepatic microcirculation disturbance induced by gut ischemia and reperfusion. *World J. Gastroenterol.* **2008**, *14*, 29–37.

(9) Zhang, W.; Wojta, J.; Binder, B. R. Effect of notoginsenoside R1 on the synthesis of tissue-type plasminogen activator and plasminogen activator inhibitor-1 in cultured human umbilical vein endothelial cells. *Arterioscler. Thromb.* **1994**, *14*, 1040–1046.

(10) Zhang, H. S.; Wang, S. Q. Notoginsenoside R1 from *Panax notoginseng* inhibits TNF-alpha-induced PAI-1 production in human aortic smooth muscle cells. *Vasc. Pharmacol.* **2006**, *44*, 224–230.

(11) Zhang, H. S.; Wang, S. Q. Notoginsenoside R1 inhibits TNF-alpha-induced fibronectin production in smooth muscle cells via the ROS/ERK pathway. *Free Radical Biol. Med.* **2006**, *40*, 1664–1674.

(12) The State Pharmacopoeia Commission of P.R. China. Radix et rhizome notoginseng. In *Pharmacopoeia of the People's Republic of China*; Chemical Industry Press: Beijing, China, 2010; Vol. I, pp 10−11.

(13) Li, X.; Wang, G.; Sun, J.; Hao, H.; Xiong, Y.; Yan, B.; Zheng, Y.; Sheng, L. Pharmacokinetic and absolute bioavailability study of total panax notoginsenoside, a typical multiple constituent traditional chinese medicine (TCM) in rats. *Biol. Pharm. Bull.* **2007**, *30*, 847–851.

(14) Li, X.; Sun, J.; Wang, G.; Hao, H.; Liang, Y.; Zheng, Y.; Yan, B.; Sheng, L. Simultaneous determination of panax notoginsenoside R1, ginsenoside Rg1, Rd, Re and Rb1 in rat plasma by HPLC/ESI/MS: platform for the pharmacokinetic evaluation of total panax notoginsenoside, a typical kind of multiple constituent traditional Chinese medicine. *Biomed. Chromatogr.* **2007**, *21*, 735–746.

(15) Liu, H.; Yang, J.; Du, F.; Gao, X.; Ma, X.; Huang, Y.; Xu, F.; Niu, W.; Wang, F.; Mao, Y.; Sun, Y.; Lu, T.; Liu, C.; Zhang, B.; Li, C. Absorption and disposition of ginsenosides after oral administration of *Panax notoginseng* extract to rats. *Drug Metab. Dispos.* **2009**, *37*, 2290–2298.

(16) Odani, T.; Tanizawa, H.; Takino, Y. Studies on the absorption, distribution, excretion and metabolism of ginseng saponins. IV. Decomposition of ginsenoside-Rg1 and -Rb1 in the digestive tract of rats. *Chem. Pharm. Bull.* (*Tokyo*) **1983**, *31*, 3691–3697.

(17) Qian, T.; Jiang, Z. H.; Cai, Z. W. High-performance liquid chromatography coupled with tandem mass spectrometry applied for metabolic study of ginsenoside Rb1 on rat. *Anal. Biochem.* **2006**, *352*, 87–96.

(18) Chang, Y. C.; Nair, M. G. Metabolism of daidzein and genistein by intestinal bacteria. *J. Nat. Prod.* **1995**, *58*, 1892–1896.

(19) Shah, P.; Jogani, V.; Bagchi, T.; Misra, A. Role of Caco-2 cell monolayers in prediction of intestinal drug absorption. *Biotechnol. Prog.* **2006**, *22*, 186–198.

(20) Artursson, P.; Karlsson, J. Correlation between oral drug absorption in humans and apparent drug permeability coefficients in human intestinal epithelial (Caco-2) cells. *Biochem. Biophys. Res. Commun.* **1991**, *175*, 880–885.

(21) Hasegawa, H.; Sung, J. H.; Matsumiya, S.; Uchiyama, M. Main ginseng saponin metabolites formed by intestinal bacteria. *Planta Med.* **1996**, *62*, 453–457.

(22) Han, B. H.; Park, M. H.; Han, Y. N.; Woo, L. K.; Sankawa, U.; Yahara, S.; Tanaka, O. Degradation of ginseng saponins under mild acidic conditions. *Planta Med.* **1982**, *44*, 146–149.

(23) Yang, L.; Xu, S.; Liu, C.; Su, Z. *In vivo* metabolism study of ginsenoside Re in rat using high-performance liquid chromatography coupled with tandem mass spectrometry. *Anal. Bioanal. Chem.* **2009**, *395*, 1441–1451.

(24) Liu, F. Y.; Wang, J. N.; Yu, S. D.; Wang, B.; Zhang, J. D. Effect of panaxatriol on hematogenesis and granulocyte-macrophage colony stimulating factor in radiation injured mice. *Saudi Med. J.* **2007**, *28*, 1791–1795.

(25) Kwok, H. H.; Ng, W. Y.; Yang, M. S.; Mak, N. K.; Wong, R. N.; Yue, P. Y. The ginsenoside protopanaxatriol protects endothelial cells from hydrogen peroxide-induced cell injury and cell death by modulating intracellular redox status. *Free Radical Biol. Med.* **2010**, *48*, 437–445.

(26) Usami, Y.; Liu, Y. N.; Lin, A. S.; Shibano, M.; Akiyama, T.; Itokawa, H.; Morris-Natschke, S. L.; Kenneth Bastow, K.; Kasai, R.; Lee, K. H. Antitumor agents. 261. 20(*S*)-Protopanaxadiol and 20(*S*)-protopanaxatriol as antiangiogenic agents and total assignment of 1H NMR spectra. *J. Nat. Prod.* **2008**, *71*, 478–481.

(27) Cui, J. F.; Bjorkhem, I.; Eneroth, P. Gas chromatographic-mass spectrometric determination of 20-(*S*)-protopanaxadiol and 20(*S*)-protopanaxatriol for study on human urinary exc retion of ginsenosides after ingestion of ginseng preparations. *J. Chromatogr., B: Biomed. Sci. Appl.* **1997**, *689*, 349–355.

(28) Hasegawa, H.; Sung, J. H.; Benno, Y. Role of human intestinal *Prevotella oris* in hydrolyzing ginseng saponins. *Planta Med.* **1997**, *63*, 436–440.

(29) Lai, L.; Hao, H.; Liu, Y.; Zheng, C.; Wang, Q.; Wang, G.; Chen, X. Characterization of pharmacokinetic profiles and metabolic pathways of 20(*S*)-ginsenoside Rh1 *in vivo* and *in vitro*. *Planta Med.* **2009**, *75*, 797–802.

Received for review February 11, 2010. Revised manuscript received April 12, 2010. Accepted April 12, 2010. The present work was supported by the Science and Technology Development Fund (Ref. No.: 049/2005/A-R1), Macau SAR, the National Basic Research Program of China (973 program, Grant No.: 2009CB522707) and the Research Committee of the University of Macau (Ref. No.: RG086/07-08S/WYT/ICMS).